Bioorganic & Medicinal Chemistry 20 (2012) 6979–6988

Contents lists available at SciVerse ScienceDirect

Bioorganic & Medicinal Chemistry

journal homepage: www.elsevier.com/locate/bmc

The interaction of nemorubicin metabolite PNU-159682 with DNA fragments d(CGTACG)$_2$, d(CGATCG)$_2$ and d(CGCGCG)$_2$ shows a strong but reversible binding to G:C base pairs

Stefania Mazzini [a,*], Leonardo Scaglioni [a], Rosanna Mondelli [a], Michele Caruso [b], Federico Riccardi Sirtori [c]

[a] DeFENS–Department of Food, Environmental and Nutritional Sciences, via Celoria 2, 20133 Milano, Italy
[b] Nerviano Medical Sciences, Oncology-Medicinal Chemistry Department, viale Pasteur 10, 20014 Nerviano (Milano), Italy
[c] Nerviano Medical Sciences,Oncology-Chemical Core Technologies Department, viale Pasteur 10, 20014 Nerviano (Milano), Italy

ARTICLE INFO

Article history:
Received 20 July 2012
Revised 11 October 2012
Accepted 14 October 2012
Available online 3 November 2012

Keywords:
Drug–DNA interactions
NMR spectroscopy
Topoisomerase inhibitors
Nemorubicin

ABSTRACT

The antitumor anthracycline nemorubicin is converted by human liver microsomes to a major metabolite, PNU-159682 (PNU), which was found to be much more potent than its parent drug toward cultured tumor cells and in vivo tumor models. The mechanism of action of nemorubicin appears different from other anthracyclines and until now is the object of studies. In fact PNU is deemed to play a dominant, but still unclear, role in the in vivo antitumor activity of nemorubicin. The interaction of PNU with the oligonucleotides d(CGTACG)$_2$, d(CGATCG)$_2$ and d(CGCGCG)$_2$ was studied with a combined use of ^{1}H and ^{31}P NMR spectroscopy and by ESI-mass experiments. The NMR studies allowed to establish that the intercalation between the base pairs of the duplex leads to very stable complexes and at the same time to exclude the formation of covalent bonds. Melting experiments monitored by NMR, allowed to observe with high accuracy the behaviour of the imine protons with temperature, and the results showed that the re-annealing occurs after melting. The formation of reversible complexes was confirmed by HPLC–tandem mass spectra, also combined with endonuclease P1digestion. The MS/MS spectra showed the loss of neutral PNU before breaking the double helix, a behaviour typical of intercalators. After digestion with the enzyme, the spectra did not show any compound with PNU bound to the bases. The evidence of a reversible process appears from both proton and phosphorus NOESY spectra of PNU bound to d(CGTACG)$_2$ and to d(CGATCG)$_2$. The dissociation rate constants (k_{off}) of the slow step of the intercalation process, measured by ^{31}P NMR NOE-exchange experiments, showed that the kinetics of the process is slower for PNU than for doxorubicin and nemorubicin, leading to a 10- to 20-fold increase of the residence time of PNU into the intercalation sites, with respect to doxorubicin. A relevant number of NOE interactions allowed to derive a model of the complexes in solution from restrained MD calculations. The conformation of PNU bound to the oligonucleotides was also derived from the coupling constant values.

1. Introduction

Nemorubicin (3′-deamino-3′-[2″(*S*)-methoxy-4″-morpholinyl] doxorubicin, (MMDX)[1,2] is a 'non conventional' anthracycline selected for clinical trials because of its novel mode of action and its important activity on tumors resistant to different classes of drugs. In particular, initial clinical studies showed the efficacy in hepatic lesions and the absence of cardiotoxic effects at optimal antitumor doses (see Scheme 1).[3]

The mechanism of action of MMDX appears different from other anthracyclines. It was shown that it works by inhibiting topoisomerase I and II,[4] and recent studies indicate also an involvement of DNA repair mechanisms in mediating its activity.[5] MMDX forms very stable complexes with DNA by intercalation into the base pairs of the double helix, with a high residence time, of an order of magnitude higher than for doxorubicin (DX), when measured with model oligonucleotides.[6,7]

In vivo, MMDX is 80–120-fold more potent than DX, but in vitro the cytotoxicity is much lower.[3] It was established[3,8] that MMDX is converted by human liver microsomes to a major metabolite, which was recognized identical to a synthetic sample of 3′-deamino-3″,4′-anhydro-[2″(*S*)-methoxy-3″(*R*)-oxy-4″-morpholinyl] doxorubicin (PNU-159682).[9] This metabolite was found to be 700–2400 fold more potent than its parent drug toward cultured human tumor cells,[3,8] and showed significant efficacy in in vivo tumor models.[10] These results suggested that PNU plays a dominant role in the in vivo antitumor activity of MMDX.[3,8]

* Corresponding author. Tel.: +39 02 50316813; fax: +39 02 50316801
E-mail address: stefania.mazzini@unimi.it (S. Mazzini).

0968-0896/$ - see front matter © 2012 Elsevier Ltd. All rights reserved.
http://dx.doi.org/10.1016/j.bmc.2012.10.033

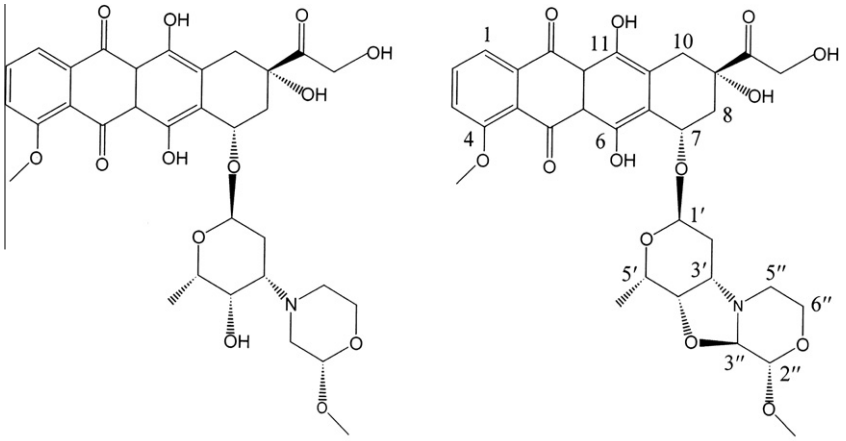

Scheme 1.

The peculiar behaviour of PNU-159682 was related[11–13] to that of the conjugates of DX and other anthracyclines with formaldehyde,[14–16] thus suggesting the formation of a covalent bond to CG-rich DNA.

No study on the interaction of this metabolite with oligonucleotides by NMR spectroscopy has been reported so far. We thought that such NMR experiments, in conjunction with Mass spectrometry analyses, could clarify the dynamics of the intercalation process and the type of binding.

The dissociation rate constants (k_{off}) of the slow step of the intercalation process can be measured with high accuracy directly by ^{31}P NMR NOE-exchange experiments[17] and do not depend upon ionic strength and self-association phenomena, as occurs for the binding constants.[6,7] The kinetic constants are an expression of the average residence time ($1/k_{off}$) of the drug in the intercalation sites. 2D-NOESY experiments allow to detect the contacts between the drug and the oligonucleotide, thus providing information on the structure of the complex. The experiments were performed with the double helix oligonucleotides d(CGTACG)$_2$ and d(CGATCG)$_2$ henceforth referred as 'TA' and 'AT' respectively. PNU-159682 is referred as PNU.

2. Results and discussion

2.1. Conformation of PNU as a free drug and in the complexes

The conformation of the drug as a free base and as a salt was deduced from the coupling constants values reported, together with those of MMDX, in the Supplementary Table S1. The results were then compared with those obtained from the data for the drug in the complexes. For the free PNU in water, as well as in $CDCl_3$ and in DMSO, the conformation of the daunosamine ring appeares similar to that of MMDX and DX.[18] The higher value of the coupling constants between H-1′ and the protons at C-2′ (5.5 and 6.0 Hz) could suggest a change of conformation, but these values are not in agreement with either a *boat* or a *twist* form, which have dihedral angles $\theta_{1',2'} = H_{1'}–C_{1'}–C_{2'}–H_{2'}$ of 180°, 60° and 90°, 30° respectively. The other couplings constants are equal to those of doxorubicins, except for $J_{3'4'}$ = 5.0 Hz and for the geminal interaction between protons at C-2′ (^2J = 15.0 Hz). The salt of PNU shows all the couplings in line with those of MMDX and DX, including $J_{1'2'}$ = 5.0 and 1.5, $J_{3'4'}$ = 3.0 and ^2J = 13.0 Hz. Therefore we think that the main factor which affects the values of the above couplings is the protonation of the amine nitrogen, and that a '*chair*' conformation of daunosamine ring is preferred also for PNU.

The morpholine ring appears more flexible. The coupling constant $J_{2''3''}$ (2.0 Hz) is the same in $CDCl_3$ and in DMSO, increases to 7.5 Hz in water for the free base and to 4.5 Hz for the salt, but those of the fragment 5″-CH_2–CH_2-6″ are almost identical in the three solvents. Among these coupling constants, one measures 9.0 Hz, typical of a diaxial interaction ($\theta_{5'',6''} \sim 180°$), the other three ones range from 3.0 to 4.0 Hz, in agreement with angles of 50–60°. The models (see Section 2.8) show that the angle $\theta_{2'',3''}$ can oscillate from 170° to 130°, without affecting the conformation of the 5″-CH_2–CH_2-6″ fragment. These angle values can justify the variation of $J_{2''3''}$ in the different solvents. Therefore the conformation of the morpholine ring appears like a '*chair*' in water, and a slightly distorted '*chair*' in the aprotic solvents. For the salt, the effect of the positive charge on the nitrogen atom may also contribute to decrease the vicinal coupling constants, with respect to the free base in water. The conformation of the morpholine ring of MMDX in water and in DMSO appears like a '*twist*', as deduced from the coupling constant values reported in Table S1 of the Supplementary.

The behaviour of PNU molecule was accurately studied in order to obtain information on the shape of the drug in the complexes, which was deduced from some coupling constants and NOE interactions. The coupling constants involving H-1′ and H-2′ of the daunosamine ring and $J_{2''3''}$ of morpholine ring are identical to those found for the PNU salt, suggesting that in the complexes the drug is protonated, even though the titration was performed with the free base. A further evidence that PNU becomes protonated in the double helix follows from the NH^+ signal (a broad doublet of 10.5 Hz) detected at 8.8 ppm and connected by TOCSY experiments to H-3″, which is a double doublet of 10.5 and 4.5 Hz. The intra-molecular NOEs, reported in Table S2 of the Supplementary together with the inter-proton distances obtained by MD (see later), were mainly used for the assignments of the proton signals of the drug in the complexes (Table S3), but they are also instrumental to establish the conformation around the glycosyl linkage. In particular, the NOE between Me-5′ of the sugar ring and one proton at C-8 of the aglycone, together with the NOEs involving OH-6 with the protons at C-1′ and C-2′ are indicative of the orientation of the daunosamine ring toward the aglycone. These NOEs were detected for both AT and TA complexes as well as for the free PNU. Thus the drug maintains its preferred conformation, that is with the methyl group Me-5′ projected toward the external side of the molecule (Fig. 1). The distance between H-8 equiv and Me-5′ protons is 4.7 Å for AT and 4.5 Å for TA complex. The torsion angles $C_7–O_7–C_{1'}–C_{2'}$ and $C_{20}–C_7–O_7–C_{1'}$ are +146° and −161° for AT, +130° and −158° for TA-complex respectively.

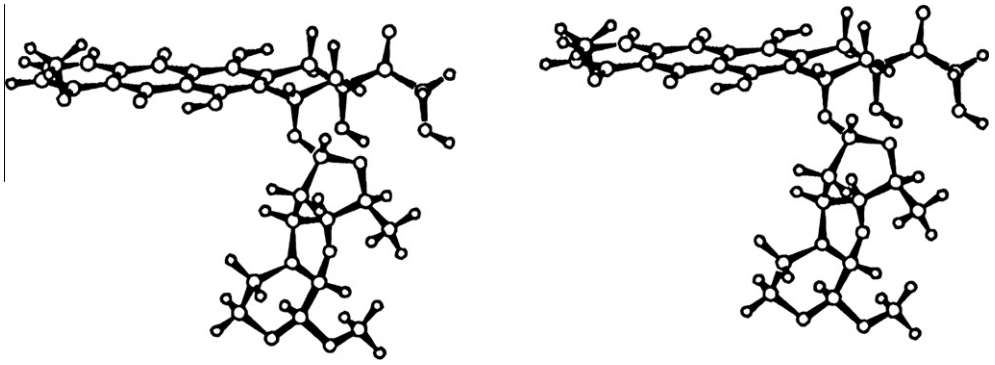

Figure 1. Stereoview of the drug in the PNU/AT complex. The torsion angles C_7–O_7–$C_{1'}$–$C_{2'}$ and C_{20}–C_7–O_7–$C_{1'}$ are +146° and −161°; $\theta_{2'',3''} = H_{2''}$–$C_{2''}$–$C_{3''}$–$H_{3''}$ is −144°, $\theta_{5'',6''} = H_{5''ax}$–$C_{5''}$–$C_{6''}$–$H_{6''ax}$ is 165°.

These values are similar to those of MMDX[7] and comparable with those of the other daunomycins,[19] as well as the conformation of the cyclohexene ring of the aglycone.

2.2. Assignment of NH and OH protons

The chelated OH protons of the drug and the imine NH protons of the base pairs lie together in the 11–13 ppm region of the NMR spectrum, but the assignment of NH vs OH was easy because the NH resonances gave sequential NOE cross-peaks and the OH signals are sharper. OH-6 was assigned vs OH-11 by the NOE interactions with H-1′ and H-2′ of the daunosamine ring. Two signals for each OH proton of the drug and four signals for each imine NH protons of the bases were observed.

We pay particular attention in detecting and assigning the geminal NH_2 protons of the bases, which lie in the 5.5–8.5 ppm region, in the free oligonucleotides and in the complexes, by performing spectra at different temperatures. The resonances of the cytidines C_1 and C_5 were always visible, whereas those of adenine and guanine G_2 sometime lack and those of G_6 could never be assigned. Adenine and guanine G_2 are the most interesting because they lie at the level of the presumed intercalation site (G_2) and close to the position where the morpholine ring should be located (A_3 and A_4). The geminal protons were first identified by TOCSY experiments, then assigned by NOE interactions: NH_2 C_1 and NH_2 C_5 with H-5 of the corresponding cytidine, NH_2 G_2 with the imine proton NHG_2C_5. The geminal protons of the adenine were always detected in both nucleotides and in their complexes and were assigned by the strong NOE with the imine NHA_3T_4 and NHT_3A_4 respectively.

The chemical shift values are reported in Tables S4 and S5 of the Supplemetary together with those obtained in the same conditions for the complexes of nemorubicin (Tables S6 and S7). A selected set of values of the AT/PNU complex is reported in Table 1.

2.3. ^{1}H NMR titration experiments

The titrations were performed with PNU as free base in different conditions (see Experimental), but in general the experiments in H_2O at 15 °C and without salts were preferred, because the portion of the spectra relative to NH and OH signals is better resolved. The increase of their resonances belonging to the bound species can easily be followed during the titration experiments. Focusing on the two resonances of OH-11 for the AT complex (Fig. 2), we can observe that for R = [PNU]/[duplex] = 0.5 to R = 1 one signal is predominant, then it decreases, while the other one increases and becomes predominant (~80–90%) for R = 3. This must be interpreted with the formation firstly of a complex with one drug and then of a complex with two drug molecules. The two signals of OH-6 are overlapped to the NH patterns and are more difficult to analyze. In principle four NH signals are expected, due to the free duplex (1 signal), to the duplex bound to one drug (2 signals) and to the duplex bound to two drug molecules (1 signal). This clearly appears from the NHG_2C_5 pattern for R = 1. We performed, for a comparison, the titration with DX and MMDX in the same conditions. (Fig. S2 in the Suplementary)

The significant upfield shift variation (0.7–1.1 ppm) found for the imine proton NHC_1G_6 and especially NHG_2C_5 (Table 1) suggests an intercalation process between the CG base pairs, as occurs for MMDX and daunomycins.[7,20] A shielding of the same order was observed for OH-6, but more modest for OH-11 (0.2–0.3 ppm). It must be noted that the shift variation of the drug molecule is less significant for two reasons: the values for the free drug are affected by the concentration and belong to the non protonated species, whereas the species into the duplex is protonated.

The complexes are symmetrical at the CG sites, as evidently appears from the pattern of the OH resonances above described. At

Table 1
Selected ^{1}H chemical shift values of $d(CGATCG)_2$ bound to PNU[a]

$d(CGATCG)_2$	Bound to PNU	$\Delta\delta$[b]
NH C_1G_6	11.98[c]	−1.13
NH G_2C_5	11.77[c], 12.85[d]	−1.08
NH A_3T_4	13.29[c], 13.58[d]	−0.35
NH_2 C_1	7.58, 6.84	−0.60, −0.22
NH_2 C_5	8.49, 6.79	−0.09, −0.23
NH_2 G_2	7.71, 6.14	−0.14, +0.07
NH_2 A_3	6.94, 5.60	−0.83, −0.38
2-H A_3	7.30[c], 7.87[d]	−0.62
8-H A_3	8.44[c], 8.18[d]	+0.15
8-H G_2	8.08[c], 7.96[d]	+0.10
8-H G_6	7.85	−0.10
6-H C_1	7.72	+0.11
6-H C_5	7.19	−0.28
6-H T_4	7.17	−0.01
5-H C_1	5.91	+0.01
5-H C_5	5.51	−0.14
Me T_4	1.24	−0.14
1′-H C_1	5.74	−0.04
1′-H G_2	6.14	+0.56
1′-H A_3	6.35	+0.05
1′-H T_4	6.16	+0.22
1′-H C_5	5.96	+0.34
1′-H G_6	5.56	−0.60

[a] Measured at 15 °C in ppm (δ) from external DSS. Solvent H_2O–D_2O (90:10 v/v), pH 6.7, R = [PNU]/[DNA] = 3, lacking data means not detected.
[b] $\Delta\delta = \delta_{bound} - \delta_{free}$; $\Delta\delta$ values for the protons of the segment from 2′-CH_2 to 5′-CH_2 are not significant.
[c] Bound species: bis-intercalated.

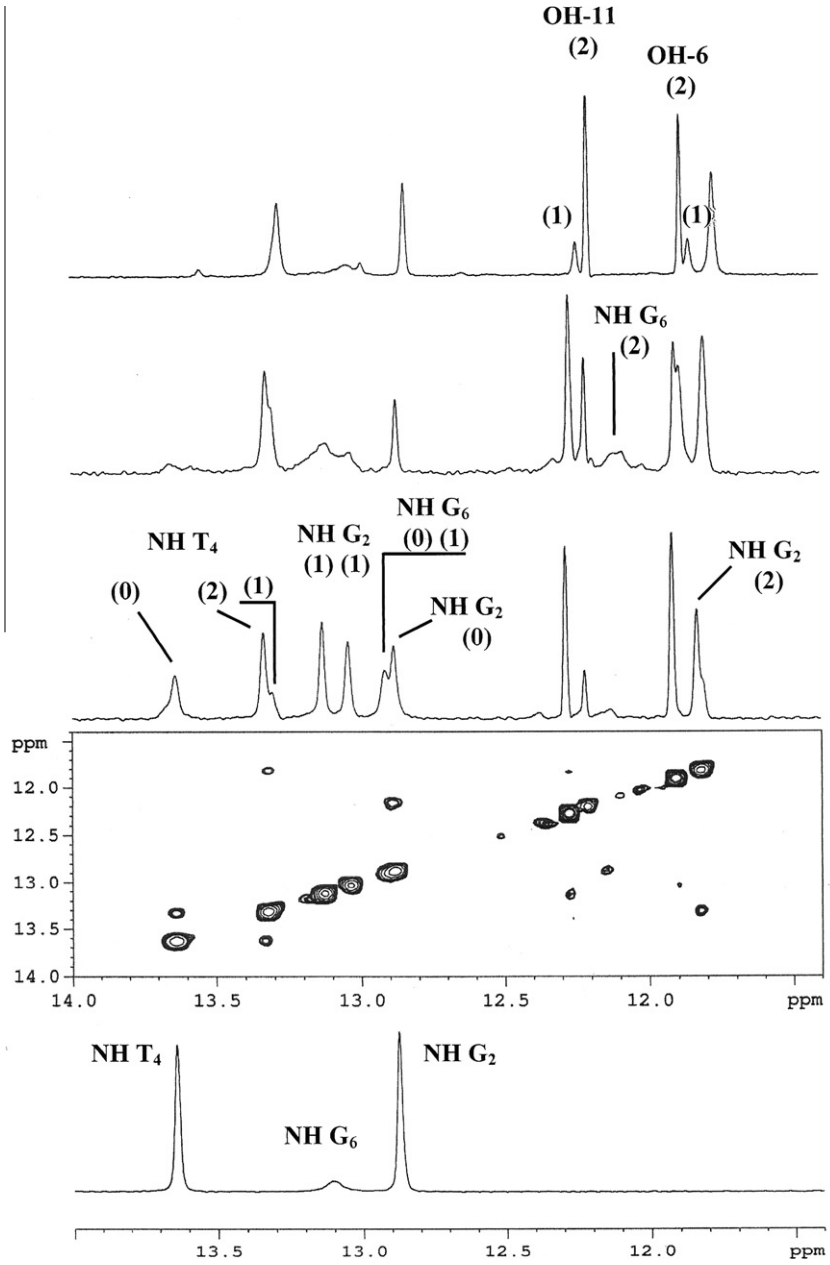

Figure 2. Low field region of the ^{1}H NMR spectra in H_2O at 15 °C, pH 6.7, of PNU/AT complex with different R = [drug]/[duplex]: (a) R = 0, (b) R = 0.75, 2D NOESY spectrum, t_{mix} = 300 ms, (c) R = 1.5, (d) R = 3.0. The resonances marked as (0), (1) and (2) belong to the free species, to the mono- and to the bis-complex, respectively.

the level of the minor groove, where the daunosamine and morpholine moieties take place (see later), the signals of H-1′, H-3′, Me-5′ and H-2″, observed in the range 15–35 °C, show that the symmetry is mantained. An excess of drug is always necessary, in order to favour the shift of the equilibrium toward the bis-intercalated species, but some amounts of mono-intercalated species and trace of free duplex are still present. The stabilization of the complexes takes some time, which in the case of the AT complex is up to one night. This can be explained with the protonation of the drug, which occurs during the interaction process with the oligonucleotide, but also with the lack of flexibility of the sugar-morpholino moiety. The evidence of a reversible process appears from the NOESY spectra, which show some exchange peaks, for instance those clearly visible in the NHA_3T_4 and NHT_3A_4 patterns (Fig. 2b) and in the aromatic protons resonances of adenine and guanines. In order to better define the exchange between the species present in solution and to study the kinetics of the process we performed phosphorus experiments.

2.4. ^{31}P NMR experiments and measurement of the kinetic constants k_{off}

The chemical shift variation of the ^{31}P resonances is the evidence of a geometrical deformation in the phosphodiester chain, generally induced by changes at the level of P-O(5′) and P-O(3′) bonds. For a B-DNA type oligomer, the values of the torsion angles α = O(3′)-P–O(5′)-C(5′) and ζ = C(3′)-O(3′)–P-O(5′) normally are −60° and −90° respectively (*gauche–gauche* conformation), whereas the *gauche-trans* conformation (α = −60°, ζ = 180°), as a consequence of intercalation, is associated with a low-field shift up to 1.0–2.5 ppm.[6,7,21–23]

The titration experiments on AT, reported in Figure ure3, shows the appearance of new signals at low field, which are connected, by 2D NOESY-exchange, with C_5pG_6 and G_2pA_3 signals of the free oligonucleotide. The NOESY spectrum is reported in the Supplementary Fig. S3. This result shows that the bound species are in a relative slow equilibrium with the free specie, and thus the interaction with the oligonucleotide leads to the formation of a reversible complex.

At low *R* values, the mono- and the bis-intercalated species were both present, as also observed in the ^{1}H NMR spectra. At high field the pattern is complicated because the A_3pT_4 and T_4pC_5 signals are partially overlapped to those of the free species. At $R = 3$ the spectrum simplifies to five rather sharp signals, due to the bis-intercalated complex, which becomes the predominant species. The assignment of these resonances (Table 2) was performed by heteronuclear 2D J-resolved experiments (Fig. S4 in the Supplementary). The resonance of G_2pA_3 of the bound species remains constant at +1.0 ppm during the titration, whereas the C_5pG_6 signal, at +0.78 ppm for $R = 0.5$, shifts progressively to low field, at +1.19 ppm for $R = 3$. The $\Delta\delta$ for both signals are +1.32 and 1.37 ppm. The resonance of A_3pT_4 moves to high field ($\Delta\delta = -0.40$ ppm) as observed for nemorubicin.[7]

The titration on TA gave similar results with the resonances at low field assigned to C_5pG_6 and G_2pT_3, but with a stronger deshielding of G_2pT_3 ($\Delta\delta = +2.15$ ppm) with respect to the AT complex.

The strong downfield shift observed in both complexes for C_5pG_6 and G_2pA_3 (G_2pT_3 respectively), indicates a deformation of the phosphorus angles at the level of CG base pairs, in agreement with the intercalation at these sites.The variation of the α and ζ torsion angles at the G_2pT_3 phosphate of TA complex appears more pronounced compared with to the angles of the G_2pA_3 phosphate in AT complex. From the models we found that the most populated conformation for PNU/TA at G_2pT_3 is *trans-gauche*, while in the PNU/AT complex, the *trans-gauche* is predominant at the C_5pG_6 phosphate. This can explain the observed stronger deshielding of G_2pT_3 phosphorus resonance in TA complex.

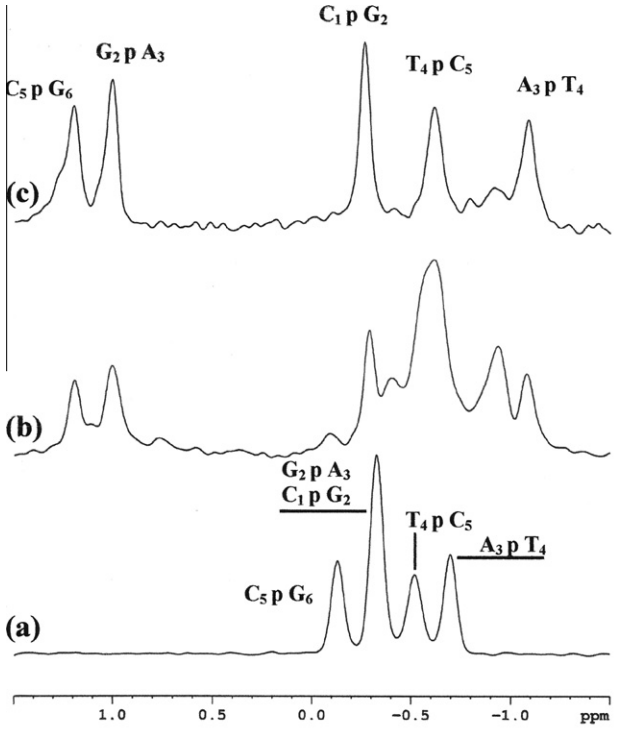

Figure 3. ^{31}P NMR spectra ^{1}H-decoupled in H_2O, pH 6.7, at 15 °C of PNU/AT complex with different *R* = [drug]/[duplex]: (a) *R* = 0, (b) *R* = 1.0, (c) *R* = 3.0.

Table 2
^{31}P chemical shift values for $d(CGATCG)_2$ and $d(CGTACG)_2$ bound to PNU[a]

Phosphate	Free duplex	Bound duplex	
Group	**AT**	δ_{bound}	$\Delta\delta$[b]
C_1pG_2	−0.32	−0.26	+0.06
G_2pA_3	−0.32	+1.00	+1.32
A_3pT_4	−0.69	−1.09	−0.40
T_4pC_5	−0.49	−0.61	−0.12
C_5pG_6	−0.18	+1.19	+1.37
	TA	δ_{bound}	$\Delta\delta$
C_1pG_2	−0.24	[c]	
G_2pT_3	−0.70	+1.45	+2.15
T_3pA_4	−0.41	−0.45	0.04
A_4pC_5	−0.47	−0.45	0.02
C_5pG_6	−0.33	+1.13	+1.46

[a] Measured at 15 °C in ppm (δ) from external MDA set at 16.8 ppm. Solvent H_2O, pH 6.7, *R* = 3.
[b] $\Delta\delta = \delta_{bound} - \delta_{free}$.
[c] Not detected.

Table 3
Dissociation rate constants (k_{off}) and averaged life time ($1/k_{off}$) for the AT- and TA-complexes with PNU, nemorubicin and doxorubicin[a]

Drug	TA-complex		AT-complex	
	k_{off} (s^{-1})	$1/k_{off}$ (s)	k_{off} (s^{-1})	$1/k_{off}$ (s)
PNU	1.50 ± 0.40	0.67 ± 0.18	0.98 ± 0.40	1.02 ± 0.38
MMDX	2.20 ± 0.06	0.45. ± 0.13	2.40 ± 1.10	0.41 ± 0.19
DX	17.3 ± 3.50	0.06 ± 0.01	23.0 ± 4.0	0.04 ± 0.01

[a] Obtained from ^{31}P spectra, at 25 °C in D_2O, 10 mM phosphate buffer, 0.1 M NaCl, pH 6.7.

As the molecular species are in a dynamic equilibrium, it was possible to measure the dissociation rate constants (k_{off}) of the slow step of the intercalation process. The data in Table 3 shows that the kinetics of the intercalation process is slower for PNU than for DX and MMDX, leading to an averaged life time ($1/k_{off}$) into the intercalation site of 1.02 s for AT and 0.67 s for TA complex respectively. These results show that the decrease of k_{off} for PNU vs DX corresponds to a 10–20-fold increase of the residence time of the drug into the intercalation sites, in line with the stronger cytotoxic activity with respect to DX, but it cannot be the only explanation for the so potent activity of PNU, toward the tumor cells, with respect to the parent drug. Many other factors may be involved in the in vivo processes to contribute to the antitumor activity. It must be noted that the measured k_{off} is related to the formation of the mono-intercalated complex, as the exchange processes are observable only for low *R* values 0.5–1.0. The residence time in the case of longer nucleotides with multiple intercalations might be significantly more important. In our model system, for instance, the bis-intercalated complexes of PNU appeared, by the melting experiments described in the following paragraph, exceptionally stable compared with those of MMDX.

2.5. Melting experiments

^{1}H NMR and UV spectroscopy were used to determine the melting point of the two oligonucleotides AT and TA, free and bound to PNU and to the parent drug MMDX. The melting points obtained by UV and NMR methods are similar, 67 °C for PNU/AT (ΔTm = 40 °C) and 60 °C for PNU/TA complex (ΔTm = 33 °C), but the phenomenon is more clearly observed by the NMR experiments, because they allow to monitor with high accuracy the behaviour of the imino protons. On lowering the temperature the re-annealing occurred, as clearly shown by the NH resonances, which reappeared at the original positions. (Fig. 4).

The UV spectra (Fig. 5 and Fig. S5), acquired monitoring the absorbance variation at 260 nm as a function of the temperature, show two transitions corresponding to the melting point of the free oligonucleotide and of the complex. The same behavour was observed[13] in the case of the interaction of PNU with d(CGCGCG)$_2$.

The solutions of the complexes were also incubated at 90 °C for 30 min and then cooled down to 25 °C. In a few hours the NMR spectra returned identical to those measured before heating, showing a perfect re-annealing.The melting experiment with the solution of MMDX/AT showed at 45 °C the disappearing of all the signals at low field including the phenolic OH of the drug (ΔTm = 10.5 °C).

This result must be interpreted with the formation of reversible complexes, which are significantly more stable in the case of PNU with respect to MMDX, the complex with AT appearing a little more stable than that with TA. The binding constant for the AT complex of PNU, is one order of magnitude higher ($K = 7.12 \pm 0.5\ 10^6\ M^{-1}$) than that found for the MMDX complex ($K = 6.85 \pm 0.3\ 10^5\ M^{-1}$), both having been obtained by UV experiments.

The fact that the duplexes are so much stabilized by PNU had induced the suggestion that a covalent bond might be formed, even if the melting experiments gave evidence for a reversible complex. The formation of a covalent bond was indeed inferred for the complex of PNU with the hexanucleotide d(CGCGCG)$_2$.[13] Thus we decided to further confirm these results by mass spectrometry, combined with endonuclease P1 digestion. This enzyme catalyzes the release of nucleotide 5′-monophosphates and the subsequent analysis by HPLC-MS allows to detect nucleotide bases covalently bound to the drug.

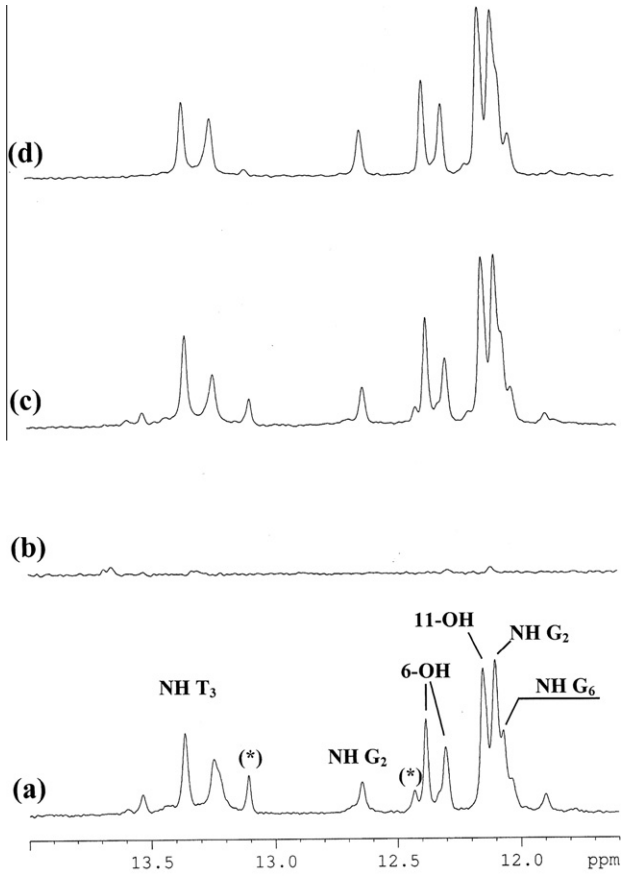

Figure 4. NH resonances of the ^{1}H NMR spectra of PNU/TA complex in H_2O, 10 mM phosphate buffer, 0.1 M NaCl, pH 6.7, with $R = 4$: (a) at 15 °C before melting, (b) at 57 °C, when melting occurs, (c) at 15 °C after melting, (d) at 15 °C after heating at 90 °C for 30 min. The resonances marked with * are assigned to the OH protons of the free PNU. They significantly decrease after heating as well as the free oligonucleotide.

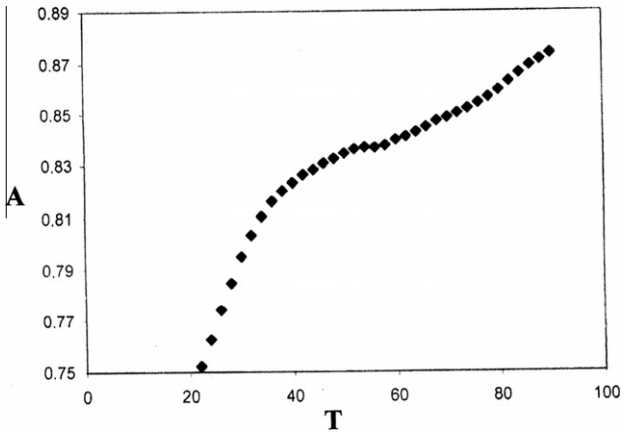

Figure 5. UV melting experiment on the PNU/TA complex in H_2O, 10 mM phosphate buffer, 0.1 M NaCl, pH 6.7, with $R = 4$.

2.6. ESI–MS and MS/MS experiments

Solutions of PNU complexes with both AT and TA oligomers ($R = 4$) already analyzed by NMR and those recovered from the melting experiments were examined by HPLC-UV/MS. The results are similar for the two complexes and are identical for samples collected before and after the melting. The HPLC pattern present, beside the signals of the free oligonucleotide and the free drug, two main peaks which showed identical mass spectra. In both cases the signal of the complex [duplex + 2 PNU]$^{3-}$ was identified at 1621 m/z. As depicted in Figure 6, the MS/MS spectrum of this complex showed the mass signal corresponding to the precursor ion [1 duplex + 2 PNU]$^{3-}$, and to the fragments [duplex + 1 PNU]$^{3-}$ and [duplex]$^{3-}$, generated by the loss of neutral PNU before the duplex dissociation into single strands. This fragmentation pathway, in MS/MS experiments, was previously described by Rosu et al.[24] for classic intercalation compounds, such as DX and daunomycin, which interact with DNA through a non-covalent mechanism. Thus this result further indicates the absence of a covalent bond between PNU and oligonucleotides.

As reported below, NMR DOSY experiments revealed the formation of [duplex + 5 PNU] and [duplex + 6 PNU] complexes at higher PNU/duplex ratio ($R = 3$). These adducts could be separated by liquid chromatography and subsequently, under mass spectrometry conditions, PNU molecules that unspecifically bind to the duplex were dissociated. As result, two peaks with a molecular weight consistent with [1 duplex + 2 PNU] complex were present in the chromatogram.

In order to obtain an additional evidence of the binding mode, the same solutions were digested with P1 endonuclease at 37 °C, pH 6.8 and pH 5.5, and then analysed by HPLC-UV/MS.[25] The spectra did not show any compound with PNU bound to the bases, but dCMP, dTMP, dC, dGMP, dAMP and free PNU (Fig. S6 in the Supplementary). These results again exclude the formation of covalent bonds and confirmed that the complexes are very stable, but the nature of the interactions is only intercalation. These experiments were performed also at neutral pH, in order to avoid a possible hydrolysis of the suggested[13] hypothetical hemiacetalic bonds between PNU and the guanine NH_2 group. On the other hand, the acetalic bond of the five-membered ring of PNU is significantly stable, as shown by the failure of the attempt to open it by the reaction with guanosine, carried out at variable temperatures untill 90 °C at neutral and acidic pH. Monitoring by NMR, this indicated that the starting materials remained unalterated.

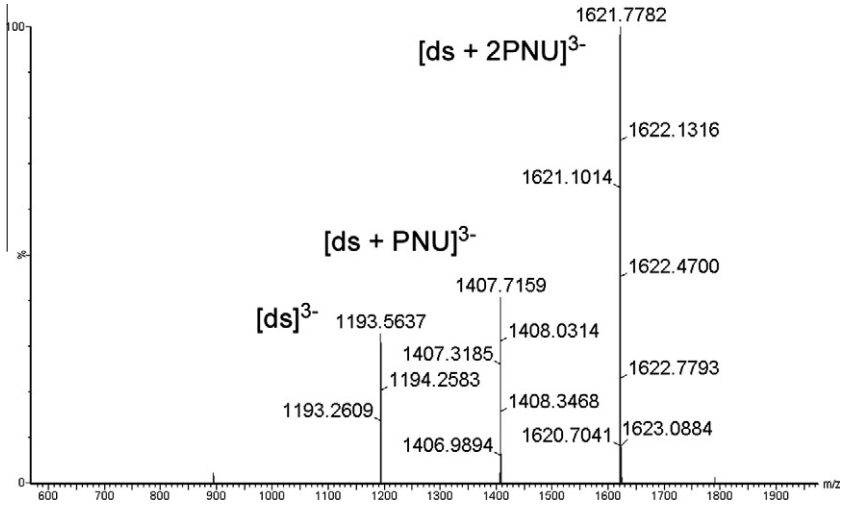

Figure 6. ESI negative ion mode MS/MS spectrum of the $[d(CGATCG)_2+2PNU]^{3-}$ complex (1621.5 *m*/*z*) at 10 V collision voltage. The spectrum corresponds to the chromatographic peak at retention time 13.3 min. (ds = $d(CGATCG)_2$).

The same experiments were performed with the hexanucleotide $d(CGCGCG)_2$. The predominant species in this case is the complex of [1 duplex + 1 PNU], but a small amount of [1 duplex + 2 PNU] is also present. The MS/MS spectra of the corresponding peaks showed the same behaviour described above for AT and TA complexes, in particular the loss of neutral PNU occurs before the denaturation of the double helix.

2.7. DOSY experiments

The NMR DOSY experiments[26] showed that, at a low concentration of PNU ($R = 0.5$), the dimension of the AT complexes present in solution corresponds to [1 duplex +1 PNU] and [1 duplex + 2 PNU]. With $R = 3$, the external aggregation becomes important, as occurs for DX[20] two values of molecular weight were obtained corresponding to [1 duplex + 5 PNU] and [1 duplex + 6 PNU]. The aggregation phenomenon appears more pronounced for TA complex: the molecular weight of the aggregate (9220) suggests the linking of two mono-intercalated duplexes through one drug molecule [2 duplexes + 3 PNU], in agreement with the lesser stability of TA complex, compared with AT complex.

2.8. NOESY experiments and modeling

The ^1H NOESY spectra of the complexes with both oligonucleotides gave a relevant number of intermolecular interactions between the ligand and the duplexes and in general the lack of the sequential intra-molecular NOEs between G_6 and C_5 protons of the nucleotides. While the strong sequential NOEs between NHA_3T_4 and NH_2G_2 and between NHG_2C_5 and NH_2A_3 observed in the AT complex, but not in the nucleotide alone, suggest the deformation of the duplex at the level of the guanine G_2 plane, that becomes closer to the adenine A_3 plane. This is also in agreement with the up field shift of H-2 and NH_2 protons of the adenine A_3 (0.6–0.8 ppm). Examples of NOESY spectra, obtained for the interaction of PNU with AT and corresponding to the 2:1 complex, are reported in the Supplementary Figures S7 and S8 and all the data are given in Table 4.

The contacts of the anthraquinone moiety with C_1 and G_6 units confirm the intercalation sites between the CG base pairs of the helix. Specifically, the orientation of the aglycone is proved by the selective interactions of the aromatic protons: H-1 and OH-11 with C_1; H-3, OMe-4 and OH-6 with G_6. But more interesting are the contacts in the minor groove, which involve the protons of the daunosamine and morpholine rings with G_2 and T_4 units. The TA

Table 4
Inter-molecular NOE interactions and inter-proton distances (Å) for the complex of PNU with $d(CGATCG)_2$[a]

PNU	$d(CGATCG)_2$	NOE[b]	d[c]
1-H	5-H C_1	w	4.8
1-H	NH_2 C_1	m	3.0
3-H	8-H G_6	s	3.8
4-OMe	2′-H G_6	s	3.9[d]
4-OMe	8-H G_6	m	4.2
6-OH	1′-H G_6	s	3.9
6-OH	8-H G_6	m	4.8
6-OH	4′-H G_6	s	3.2
8-CH_2	1′-H G_6	m[e]	4.2[f]
11-OH	6-H C_1	s	3.8
11-OH	5-H C_1	m	4.3
11-OH	1′-H G_2	m	4.8
11-OH	2′-H C_1	s	2.4[d]
11-OH	NH G_2C_5	m	4.8
11-OH	NH_2 C_1	m	5.1
3′-H	NH G_2C_5	m	4.4
3′-H	NH_2 G_2	s	2.2
3′-H	1′-H G_2	w	4.4
5′-H	NH_2 G_2	m	4.5
5′-Me	1′-H G_2	s	4.3
2″-H	1′-H T_4	w	5.1
2″-H	NH_2 G_2	s	3.0
3″-H	1′-H G_2	m	4.9
6″-CH_2	1′-H T_4	s	3.5
6″-CH_2	NH A_3T_4	s	4.4
Relevant conformational energy parameters			
E(Kcal/mol)			
Forcing		+22.2	
Van der Waals		−635.3	
Hydrogen-bond		−10.7	
Coulomb		−107.0	
Total		−150	
Distance violations (>0.3 Å)		4[g]	

[a] Acquired at 10, 15 and 25 °C. Solvent H_2O–D_2O (90:10 v/v), pH 6.7. R = [drug]/[duplex] = 3.
[b] A quantification of the NOE intensities were estimated as follow: $s = 2.5–3.5$, $m = 3.5–4.5$, $w = 4.5–5.5$ Å.
[c] Obtained from the final structure of the complex after MD calculations. For NH_2, for methyl and methylene groups the distance is referred to the closest proton.
[d] The distance is referred to the *pro-S* proton.
[e] Partially secondary NOE through H-7 ($d = 3.3$ Å); H-7 is overlapped by H_2O.
[f] The distance is referred to the axial proton.

complex present analogous interactions of the aglycone moiety with C_5 and G_6, and of the sugar and morpholine protons with A_4 and G_6. The NOE data are reported in Table S8 of the Supplementary.

We developed a model for PNU and for both complexes with one intercalated PNU molecule, by docking the PNU molecule into the double helix in an orientation that qualitatively satisfies the NOE values. The orientation of the intercalating aglycone moiety, as said before, is similar for both complexes. This appears from the distance between the anthraquinone ring and the second base pairs G_2C_5, as well as from the distance between the two strands of the double helix. The models of the complexes are reported in Figure 7.

Small differences in the two complexes arise from the orientation of the daunosamine moiety and from the position of the morpholine ring, which protrudes in the minor groove. This is due to a sum of small differences between the conformations of the rings and between the values of the torsion angles φ and ψ around the glycosidic bond, found in the two complexes. The sugar moiety in the AT complex is located closer to the 3′–5′ strand, as proved by the NOEs interactions of H-3′, H-5′ and Me-5′ with the G_2 unit. At the level of the morpholine ring, H-3″, H-2″ and 6″-CH_2 protons gave interactions with G_2 and T4 residues. On the contrary, in the TA complex, the sugar and morpholino moieties lie closer to the 5′–3′ strand, as shown by the NOE contacts of daunosamine protons with G_6 and of the morpholino protons with A_4 unit respectively. The different position of the drug in the minor groove observed in the models can explain the different $\Delta\delta$ values found for H-1′ of G_2 and G_6 in the two complexes. But the most significant observation is the finding that in the AT complex a strong NOE occurs between one proton of the G_2 amino group and H-3′ (d = 2.2 Å), interaction which was not detected in the TA complex (d = 4.5 Å as measured in the model). In the AT complex, also H-2″ presents a similar interaction with one amino proton of G_2, which is then transmitted (secondary NOE), via the other geminal proton of the NH_2 group, to the imine NHG_2C_5 resonance. This is a consequence of the different sequence of the two nucleotides: the presence of the triplet CGA appears to favour this geometry and thus the positive charge of the NH^+ bound to C-3′ can better interact with the electron-rich NH_2 group of the guanine. This could then explain the enhanced stability of the AT with respect to the TA complex.

The preference for CGA with respect to CGT sequence was also found for DX and daunomycin and explained with the presence of the H-bond between 3′-NH_3^+ and O-2 of T_4 observed in the X-ray structure.[27] In our AT/PNU model such H-bond does not take place because the distance is 6.4 Å. The H-bond between OH-9 of the aglycone and N-3 and NH_2 of G_2, found in the X-ray of DX[27] and MMDX[28,29], was said to contribute to stabilize the complexes. In our model of AT complex the distances between OH-9 and N-3 and NH_2 of G_2 are too large (5.8 and 4.7 Å) for possible H-bonds. The complexes with MMDX should be further stabilized by the interactions of the morpholine and sugar rings into the minor groove: in AT complex[29] the C-3″ atom was found 3.76 Å to C-2 of adenine A_3, while in the TA complex C-3″ is 4.26 Å to the adenine of the opposite strand. Short distances between H-3′ or H-3″ and NH_2 of G_2 were not found in the above X-ray structures.

3. Conclusions

The formation of covalent bonds between PNU and CG-rich DNA has been suggested[11,13] to explain the potent activity toward tumor cells of nemorubicin through its metabolite. The aim of this study was to elucidate the details of the DNA-interaction, the nature of the complexes and thus confirm the existence of covalent bonds between PNU and model oligonucleotides. However, our experiments do not support the hypothesis of a covalent bond, even if we can not exclude that it may occur in vivo.

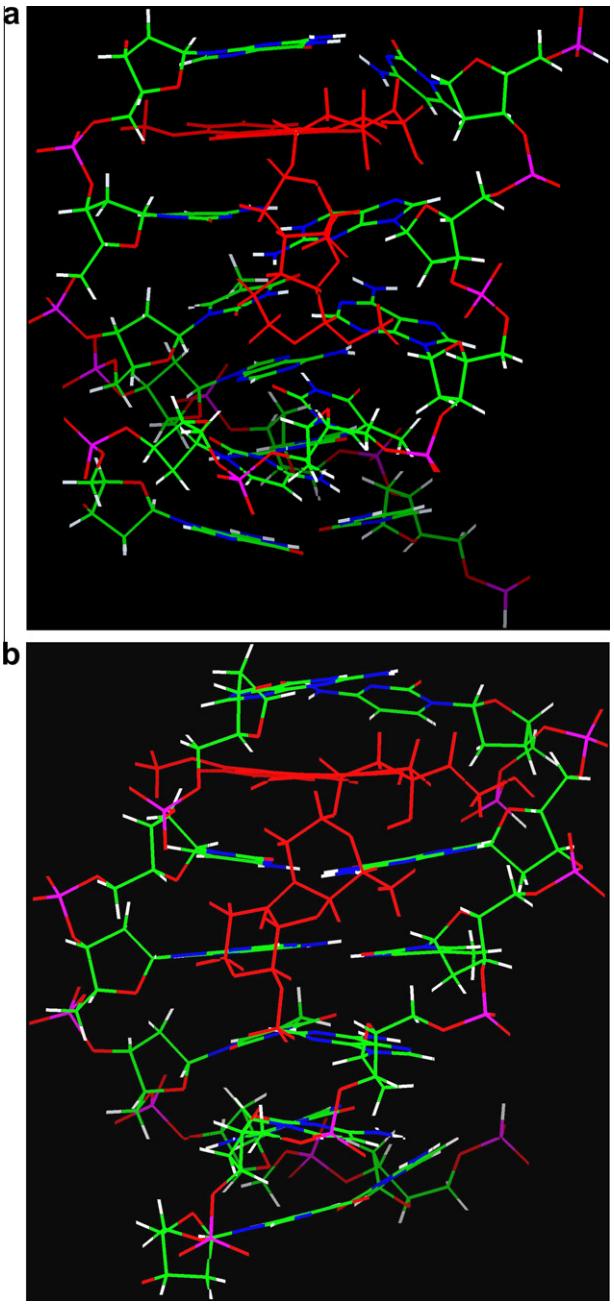

Figure 7. Energy minimized molecular models of the mono-intercalated complexes: (a) PNU/AT and (b) PNU/TA.

PNU intercalates between the CG base pairs of the helix like other anthracyclines of this series, but the stability of the complexes is much higher. This follows not only from the binding constant, which is one order of magnitude higher than that of nemorubicin, but rather from the melting experiments. The binding constants are known to be affected by many factors (for instance aggregation phenomenona) also during UV measurements, whereas melting experiments, if performed by NMR, are particularly accurate. This is because NMR allows to directly observe the imine protons and so to monitor their behaviour as a function of the temperature. The melting experiments showed a significant increment of the ΔTm value for PNU compared to MMDX, but also a perfect re-annealing after melting, which is evidence of a reversible process.

This is confirmed by mass spettrometry experiments, also combined with endonuclease P1 digestion. The MS/MS spectra showed the loss of neutral PNU before the breaking of the double helix, a behaviour typical of intercalators. Then, after digestion with the enzyme, the spectra did not show any compounds with PNU bound to the bases, but dCMP, dTMP, dC, dGMP, dAMP, and free PNU.

The evidence of a reversible process also comes from the proton and phosphorus NOESY spectra of PNU complexes with $d(CGTACG)_2$ and $d(CGATCG)_2$. The dissociation rate constants (k_{off}) of the slow step of the intercalation process, measured by ^{31}P NMR NOE-exchange experiments, showed that the kinetics of the process is slower for PNU than for doxorubicin and nemorubicin, leading to a 10–20-fold increase of the residence time of PNU into the intercalation sites, compared to DX. This is in line with the stronger cytotoxic activity with respect to DX, but it can not be the only explanation for the so potent activity of PNU toward the tumor cells compared to the parent drug. Actually many factors are indeed responsible for the antitumor activity. The residence time, in the case of longer nucleotides with multiple intercalations might be significantly more important. In our model system, for instance, the bis-intercalated complexes of PNU appeared, by the melting and mass experiments, exceptionally stable compared with those of MMDX. In PNU complexes the drug is protonated, even though the titration was performed with the free base. This explains the fact that the stabilization of the complexes takes some time, as much as overnight.

A relevant number of NOE interactions allowed a model of the complexes in solution to be derived through restrained MD calculations. Small differences in the AT and TA complexes arise from the orientation of the daunosamine moiety and from the position of the morpholine ring, which protrudes in the minor groove. The sugar in the AT complex is located closer to the 3′–5′ strand, whereas in the TA complex, the sugar and morpholine moieties lie closer to the 5′–3′ strand. In the AT complex, the daunosamine 3′-NH^+ is close to the NH_2 group of guanine G_2. This is a consequence of the different sequence of the two nucleotides. The presence of the triplet CGA appears to favour this geometry, which allows the positive charge of 3′-NH^+ to interact with the electron-rich NH_2 group of the guanine. This could then explain the enhanced stability of the AT with respect to the TA complex.

4. Experimental

4.1. Sample preparation

The oligonucleotides, purified by HPLC, were purchased from Primm (Milan, Italy) and dissolved in D_2O or in H_2O/D_2O (90:10 v/v) at a 0.5–1 mM concentration range, in the absence or in the presence of 100 mM or 20 mM of NaCl and 10 mM phosphate buffer, pH 6.7. PNU samples were obtained from Nerviano Medical Sciences as free base. We decided to use the free base for all the experiments in order to be sure of the stability of the compound and also because the drug in this form was used for the biological and clinical tests. As the free base is insoluble in water, 1.2 mg/2.1 mg of the drug were dissolved in 200 ml of DMSO, [9.3 mM/16 mM]. This solution was used for each titration experiments. Before the titration experiments, the NMR spectrum in water of PNU was analyzed in the same conditions, as a free base and as a salt. The salt was obtained with a trace of gaseous HCl directly in the NMR tube.

4.2. UV experiments

UV spectra were recorded with a Jasco V-560 spectrophotometer in 10 mM sodium phosphate buffer, 20 mM NaCl, pH 6.7 with a sample concentration of 10^{-6} M, in the absence and in the presence of the drug at a ratio R = [drug]/[duplex] = 2.0. Temperature-ramp experiments were performed by using a software-driven, Peltier-based temperature controller gradient (0.5 °C/min). Fixed wavelength measurements were taken at 260 nm from 6 to 80 °C. All the measurements were repeated twice and the variation of the melting temperature due to the drug has been derived. The equilibrium constants were determined following the reported[30] protocol and equations.

4.3. NMR experiments

The NMR spectra were recorded on a Bruker AV600 spectrometer operating at a frequency of 600.10 MHz and 242.94 MHz, for ^1H, and ^{31}P nuclei respectively. ^1H and ^{31}P spectra (broad-band ^1H decoupled mode) were recorded at variable temperature ranging from 5 to 70 °C. Chemical shifts (δ) were measured in ppm. ^1H and ^{31}P NMR spectra were referenced respectively to external DSS (2,2-dimethyl-2-silapentane-5-sulfonate sodium salt) set at 0.00 ppm and MDA (methylenediphosphonic acid) set at 16.8 ppm. Estimated accuracy for protons is within 0.02 ppm, for phosphorus is within 0.03 ppm.

^1H NMR titrations were performed at pH 6.7 and at different temperatures, but the best results were obtained at 15 °C and 10 °C, by adding increasing amounts of the drug to the oligonucleotide solution in H_2O/D_2O until R = [drug]/[duplex] = 4.0 was reached. ^{31}P NMR titrations were performed in D_2O and in H_2O at 25, 15 and 5 °C. ^1H assignments for the drugs were performed by using NOESY and TOCSY experiments. The sequential assignments in free and bound oligonucleotides were performed by applying well established procedures for the analysis of double stranded B-DNA.[31] All the protons of the bound species were attributed (data reported in the Supplementary data). The ^1H and ^{31}P assignments for the free oligonucleotides $d(CGTACG)_2$ and $(CGATCG)_2$ have previously been reported.[32–34]

The melting experiments were performed by using ^1H NMR spectroscopy at variable temperature in H_2O/D_2O solutions without salts.

Phase sensitive NOESY spectra were acquired at 25, 15 and 10 °C in TPPI mode, with 4 K times 512 complex FIDs, spectral width of 8400 and 15.000 Hz for D_2O and H_2O solutions respectively, recycling delay of 1.5 s, 120 scans. Mixing times ranged from 50 to 300 ms. The experiments were performed on all the solutions from R = 1 to R = 4. The NOE data reported in Table 4 were obtained with R = 3, corresponding to a 2:1 complex. TOCSY spectra were acquired with the use of a MLEV-17[35] spin-lock pulse (field strength 10.000 Hz, 60 ms total duration). All spectra were transformed and weighted with a 90° shifted sine-bell squared function to 4 × 1 K real data points. For samples dissolved in D_2O, water suppression was achieved by pre-saturation. For samples in H_2O, the 3–9–19 and the excitation sculpting sequences from standard Bruker pulse program libraries were employed. ^{31}P-2D-NOESY exchange experiments[17] were acquired (2 K × 320 FIDs, 420 scans) at different mixing times ranging from 50 to 300 ms. The value of k_{off} results by fitting of the experimental data on the following equations :

$$I_{AA} = 1/2[1 + \exp(-2kt_{mix})]\exp(-t_{mix}/T_1^A)M_{A0}$$

$$I_{AB} = 1/2[1 - \exp(-2kt_{mix})]\exp(-t_{mix}/T_1^B)M_{B0}$$

Where I_{AA} and I_{AB} are the intensities of diagonal and cross peaks respectively, t_{mix} is the mixing time and M_{A0}, M_{B0} are the equilibrium magnetizations. T_1^A and T_1^A are the longitudinal relaxation times of phosphates at the site A and B. Heteronuclear 2D J-resolved spectra were acquired by the proton-flip method[36], using the pulse sequence HET2DJ included in the spectrometer library.

Pseudo two-dimensional DOSY[26] experiments were acquired using the pulse-program 'stebpgp1s', diffusion delay: 0.12–0.45 s; gradient pulse: 1.5 ms; number of increments: 64. Raw data were processed using the standard DOSY software present in the Bruker library (TOPSPIN v. 1.3). A calibration curve was obtained using, as standards, samples with a range of MW from 180 to 23.500, as reported.[20]

4.4. Molecular modeling

Molecular models of $d(CGTACG)_2$, $d(CGATCG)_2$ and PNU were built with Insight II & Discover (version 97.0 MSI, San Diego, CA) on a Silicon Graphics O2 workstation, using standard fragments from the Silicon Graphics library. The AMBER36 force-field was utilized without explicit inclusion of solvent molecules, setting a distance-dependent relative permittivity $e = 4.0$ r and scaling the 1–4 non bond interactions by a factor of 0.5. For drugs, partial atomic charges were calculated using MOPAC37 and the potentials were set by similarity with the DNA aromatic and sugar atoms. The drug-DNA complexes were then constructed following the NOE interactions. The models were energy minimized and then a 100 ps of restrained MD simulation was performed at a constant temperature of 300 K sampling the trajectory every picosecond. As restraints the hydrogen bonds between helical base pairs (except terminal base pairs) and the drug-DNA interproton distances were applied.

4.5. MS experiments

HPLC-MS and MS/MS experiments were performed by using a Q-TOF Ultima (Waters, Manchester, UK) mass spectrometer operating in negative ion mode and connected to a 1100 μ-HPLC system (Agilent, Palo Alto, US).

Analyses were performed on a column XTerra MS C18 column 1.0 × 50 mm, 2.5 μm particle size (Waters, Milford, US) with mobile phase A HFIP (0.1 M)/TEA pH 8.2 and methanol (mobile phase B). (95% A → 50% A over 25 min, 50% A for 5 min, flow rate 40 μL/min).

Solutions of PNU with both AT and TA oligomers (R = [drug]/[DNA] = 4.0) were digested as previously described.[25] Enzymatic digestion was done on DNA solution 30 μM using nuclease P1 2 U/mL (Sigma–Aldrich, St. Louis, US) in 20 mM ammonium acetate buffer (pH 5.5 and 6.8) with 500 μM $ZnCl_2$. Samples were incubated at 37 °C for 12 h. Ten microliters of this solution were directly analyzed by HPLC-MS/UV on a LCQ (Thermo, San Jose, US) ion trap instrument, equipped with an electrospray ion source, connected to a P4000 HPLC pump with UV6000LP diode array detector (TSP, San Jose, US). A Waters Atlantis dC18 column 150 × 4.6 mm, 5 μm particle size was used. Mobile phase A was ammonium acetate 5 mM buffer (pH 5.5 with acetic acid), and mobile phase B was methanol (100% A for 10 min, 100% A → 10% A over 10 min, 10% A for 2 min, flow rate 1 mL/min).

Acknowledgments

This work was supported by the University of Milano (PUR09) and by MIUR (Funds PRIN09).

Supplementary data

Supplementary data associated with this article can be found, in the online version, at http://dx.doi.org/10.1016/j.bmc.2012.10.033.

References and notes

1. Bargiotti, A.; Zini, P.; Penco, S.; Giuliani, F. US Patent 4,672,057, 1987.
2. Grandi, M.; Pezzoni, G.; Ballinari, D.; Capolongo, L.; Suarato, A.; Bargiotti, A.; Faiardi, D.; Spreafico, S. *Cancer Treat. Rev.* **1990**, *17*, 133.
3. Quintieri, L.; Fantin, M.; Palatini, P.; De Martin, S.; Rosato, A.; Caruso, M.; Geroni, C.; Floreani, M. *Biochem. Pharmacol.* **2008**, *76*, 784. and references quoted.
4. Lau, D. H. M.; Duran, G. E.; Lewis, A. D.; Sikic, B. I. *Br. J. Cancer* **1994**, *70*, 79.
5. Sabatino, M. A.; Marabese, M.; Ganzinelli, M.; Caiola, E.; Geroni, C. *Mol. Cancer* **2010**, *9*, 259.
6. Bortolini, R.; Mazzini, S.; Mondelli, R.; Ragg, E.; Ulbricht, S.; Vioglio, S.; Penco, S. *Appl. Magn. Reson.* **1994**, *7*, 71.
7. Mazzini, S.; Mondelli, R.; Ragg, E. *J. Chem. Soc., Perkin Trans. 2* **1998**, 1983.
8. Quintieri, L.; Geroni, C.; Fantin, M.; Battaglia, R.; Rosato, A.; Speed, W.; Zanovello, P.; Floreali, M. *Clin. Cancer Res.* **2005**, *11*, 1608.
9. Caruso, M.; Lovisolo, P.; Geroni, C.; Suarato, A. Eur. Pat. 0,889,898 B1, 2002.
10. Yuan, S.; Zhang, X.; Lu, L.; Xu, C.; Yang, W.; Ding, J. *Anticancer Drugs* **2004**, *15*, 641.
11. Antunes, J.L.; Gatto, B.; Quintieri, L.; Floreali, M.; Geroni, C. *J. Chemotherapy*, **2004**, *16*, Suppl. n.1, 155, *Abstracts of Papers*, 1st Intern. Conference on Cancer Therapeutics, Florence, 2004.
12. Scalabrin, M.; Quintieri, L.; Palumbo, M.; Gatto, B. *Abstract of Papers*, XIX National Meeting on Medicinal Chemistry, Verona, 2008.
13. Scalabrin, M. Ph.D Thesis, University of Padova, 2011.
14. Wang, A. H. J.; Gao, Y. G.; Liaw, Y. C.; Li, Y. K. *Biochemistry* **1991**, *30*, 3812.
15. Fenich, D. J.; Taatjes, D. J.; Koch, T. H. *J. Med. Chem.* **1997**, *40*, 2452.
16. Colwell, K. E.; Cutts, S. M.; Ognibene, T. J.; Henderson, P. T.; Phillips, D. R. *Nucleic Acids Res.* **2008**, *36*, e100.
17. Bodenhausen, G.; Ernst, R. R. *J. Am. Chem. Soc.* **1982**, *104*, 1304.
18. Mondelli, R.; Ragg, E. *J. Chem. Soc., Perkin Trans. 2* **1987**, 15.
19. Mondelli, R.; Ragg, E. *J. Chem. Soc., Perkin Trans. 2* **1987**, *2*, 27.
20. Mazzini, S.; Scaglioni, L.; Animati, F.; Mondelli, R. *Bioorg. Med. Chem.* **2010**, *18*, 1497.
21. Ragg, E.; Mondelli, R.; Battistini, C.; Garbesi, A.; Colonna, F. P. *FEBS Lett.* **1988**, *236*, 231.
22. Gorenstein, D. J. *Chem. Rev.* **1994**, *94*, 1315.
23. Precechtelova, J.; Novak, P.; Munzarova, M. L.; Kaupp, M.; Sklenar, V. *J. Am. Chem. Soc.* **2010**, *132*, 17139.
24. Rosu, F.; Pirotte, S.; De Pauw, E.; Gabelica, V. *Int. J. Mass Spectrom.* **2006**, *253*, 156.
25. Shimelis, O.; Giese, R. W. *J. Chromatogr., A* **2006**, *1117*, 132.
26. Morris, K. F.; Johnson, C. S., Jr. *J. Am. Chem. Soc.* **1992**, *114*, 3139.
27. Moore, M. H.; Hunter, W. N.; Langlois d'Estaintot, B.; Kennard, O. *J. Mol. Biol.* **1989**, *206*, 693. and references quoted.
28. Cirilli, M.; Bachechi, F.; Ughetto, G.; Colonna, F. P.; Capobianco, M. L. *J. Mol. Biol.* **1992**, *230*, 878.
29. Gao, Y.; Wang, A. H.-J. *J. Biomol. Struct. Dyn.* **1995**, *13*, 103.
30. Marky, L. A.; Breslauer, K. J. *Biopolymers* **1987**, *26*, 1601.
31. Neuhaus, D.; Williamson, M. *The Nuclear Overhauser Effect in Structural and Conformational Analysis*; VCH: New York, 1998.
32. Delepierre, M.; Huynh Dihn, T.; Proques, B. P. *Biopolymers* **1989**, *28*, 2115.
33. Lown, J. W.; Hanstock, C. C.; Bleackley, R. C.; Imbach, J. L.; Rayner, B.; Vasseur, J. J. *Nucleic Acids Res.* **1984**, *12*, 2519.
34. Ragg, E.; Mondelli, R.; Battistini, C.; Vioglio, S. *Magn. Reson. Chem.* **1989**, *27*, 640.
35. Bax, A.; Davis, D. G. *J. Magn. Reson.* **1985**, *65*, 355.
36. Sklenar, V.; Bax, A. *J. Am. Chem. Soc.* **1987**, *109*, 7525.